Large Deformation Simulation of Anisotropic Material

R.H.W. ten Thije, R. Akkerman, J. Huétink

University of Twente, Composites Group - CTW/OPM/PT, P.O. Box 217, 7500 AE Enschede, the Netherlands
URL: www.opm.ctw.utwente.nl/research/pt e-mail: R.H.W.tenThije@utwente.nl

ABSTRACT: Large deformation Finite Element (FE) simulations of anisotropic material often show slow convergence or break down with increasing anisotropy and deformation. Large deformations are generally approximated by multiple small linearised steps. This leads to poor performance and contradicting formulations. Here, a new conceptually simple scheme was implemented in an updated Lagrange formulation. An appropriate decomposition of the deformation gradient results in constitutive relations defined in invariant tensors such as the right Cauchy-Green tensor. Consistent tangent matrices are given for a linearly elastic fibre model and for a generalized anisotropic material. The simulations are robust, showing quadratic convergence for arbitrary degrees of anisotropy and arbitrary deformations with strain increments over 100%.

Key words: finite element simulation, anisotropy, large deformation

1 INTRODUCTION

Numerical optimization of products and production processes becomes increasingly important in the design phase of composite structures. It can reduce the time to market and can avoid the production of costly prototypes. Numerical simulations of the forming processes such as e.g. draping, rubber pressing or diaphragm forming are an essential part of these optimization tools.

Finite Element (FE) simulations are capable of simulating the production process in great detail, including mechanisms such as tool-part friction, inter-ply friction, wrinkling and fibre bridging. These FE simulations are however time consuming and often not very robust. Large deformation FE simulations of anisotropic material often show slow convergence or break down with increasing anisotropy and deformation.

1.1 Uniaxial tensile test

A simulation of a simple tensile test with a ply of unidirectional fibres reveals the difficulties when using a standard FE formulation. The material is highly anisotropic with a stiffness ratio of 1 to 10^5. An arbitrary commercial FE code, ANSYS, is used to simulate the experiment. Plane stress quadrilaterals (PLANE42) are used. The left and right side are clamped and the right side moves in the *y*-direction (*see figure 1*). The incremental displacement δ is very small, only $5 \cdot 10^{-5}$ times the length of the specimen. Nevertheless, the simulation breaks down after only 4 steps at an elongation of only 0.02%. Figure 1 shows the last converged solution.

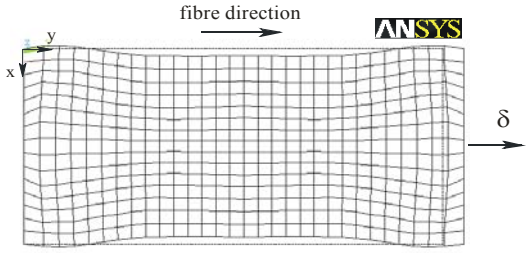

Fig. 1. Deformed shape (x250) tensile test simulation with a highly anisotropic material.

The ply widens near the clamped edges, while it should contract due to the Poisson effect.
This is caused by updating the material orientations using the wrong geometry. Element strains ε are found by:

$$\varepsilon = B \cdot u \,, \tag{1}$$

where B contains the derivatives of the element shape functions and u denotes the nodal displacements. Implicit codes obtain the highest order of convergence if B is evaluated on the intermediate geometry between the initial state and the current deformed state. The resulting stresses and subsequently the nodal forces become misaligned if the material orientation is updated using the same intermediate geometry, as illustrated in figure 2b.

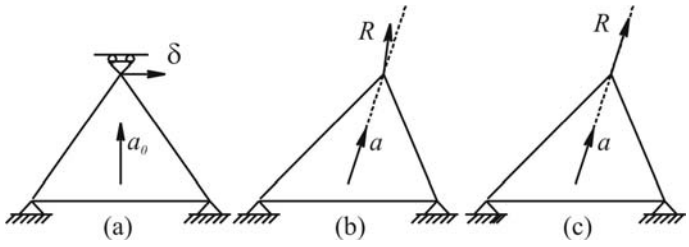

Fig. 2. Resulting (mis-) alignment of the nodal force

The orientation update should take place using the current geometry to avoid misalignment of the nodal forces in large deformation simulations with anisotropic material (c).

1.2 Pure shear

Incorrect deformed shapes can be avoided by evaluating the material tensor using the final geometry. Unfortunately this leads to less accurate strain predictions as shown in the next example. One element is sheared up to 75°. Applying pure shear should not introduce strains in the fibres which are aligned with the frame. Figure 3 shows a fibre strain of 0.3 [-], evaluated according to equation (1), if the deformation is applied in one step. The accuracy improves if the total deformation is split into several steps, but this increases the calculation time significantly. As much as 86 steps are necessary to reduce the fibre strain below 1%.

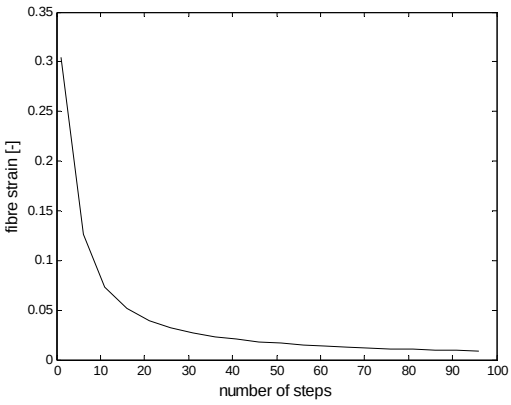

Fig. 3. Inaccurate fibre strain in pure shear

The 'standard' large deformation simulations are based on the assumption that a large nonlinear displacement can be accurately approximated by multiple small steps in which a linear theory is applied. This assumption leads to poor performance in implicit FE simulations with (highly) anisotropic material. The previous examples illustrate that it leads to contradicting requirements as well. A review of the Finite Element formulation is necessary if large deformations of anisotropic material are considered.

2 LARGE DEFORMATION THEORY

Figure 4 shows a volume of material in the undeformed or initial state and in the deformed or current state. The deformation gradient ***F(X,t)*** maps the initial configuration onto the current configuration and can be decomposed in a stretch tensor ***G*** and a subsequent rotation ***R***:

$$\boldsymbol{F} = \boldsymbol{R} \cdot \boldsymbol{G} \tag{2}$$

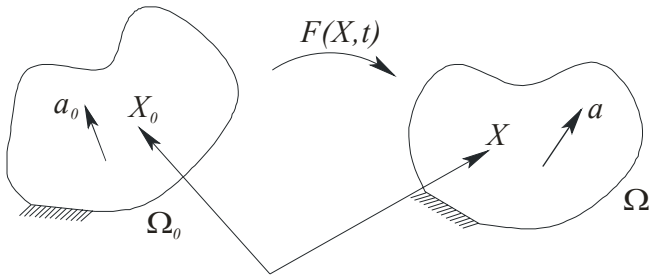

Fig. 4. Initial and current configuration of a body.

This decomposition is not unique and ***G*** does not necessarily have to be symmetric. In case of a one dimensional fibre it is convenient to take a rotation ***R*** that rotates the initial fibre direction $\boldsymbol{a}_0$ to the current fibre direction ***a***. The non-symmetrical tensor ***G*** now relates the current length ℓ to the original length ℓ_0.

$$\boldsymbol{a} = \boldsymbol{F} \cdot \boldsymbol{a}_0, \quad \boldsymbol{R} \cdot \boldsymbol{a}_0 = \frac{\ell_0}{\ell}\boldsymbol{a}, \quad \boldsymbol{G} \cdot \boldsymbol{a}_0 = \frac{\ell}{\ell_0}\boldsymbol{a}_0 \tag{3}$$

2.1 Invariancy of the local stress tensor

The local stress tensor $\boldsymbol{\tau}$ is **invariant** and related to the Cauchy stress tensor $\boldsymbol{\sigma}$ through the following relation:

$$\boldsymbol{\sigma} = \boldsymbol{R} \cdot \boldsymbol{e}_i \tau_{ij} \boldsymbol{e}_j \cdot \boldsymbol{R}^T \tag{4}$$

with $\boldsymbol{e}_i$ and $\boldsymbol{e}_j$ the local base vectors. These local base vectors co-rotate with the materials axes of anisotropy and allow for constitutive equations in terms of an **invariant** and **constant** material tensor *E*. There is no need for non-orthogonal constitutive equations as introduced by Yu [2] and Xue [3].
This approach leads to a conceptually simple scheme for an updated or total Lagrange formulation and is introduced by Huétink [1]. Nonlinearities due to reorientation of the material are taken into account when mapping the local stress tensor to the global Cauchy stress tensor.
The rate of the Cauchy stress is necessary to assemble the element stiffness matrix. This rate is related to the local stress tensor by:

$$\dot{\boldsymbol{\sigma}} = \dot{\boldsymbol{R}} \cdot \boldsymbol{\tau} \cdot \boldsymbol{R}^T + \boldsymbol{R} \cdot \dot{\boldsymbol{\tau}} \cdot \boldsymbol{R}^T + \boldsymbol{R} \cdot \boldsymbol{\tau} \cdot \dot{\boldsymbol{R}}^T \tag{5}$$

The next step is to find the local stress $\boldsymbol{\tau}$ as a function of an appropriate strain measure.

2.2 Strains and stresses

The *right Cauchy-Green tensor* ***C*** equals unity if no deformation takes place and is invariant under rigid body rotations. Huétink [1] showed that the free energy can be expressed as a function of ***C*** only, whereas that is not possible for the *left Cauchy-Green tensor* ***B*** in case of anisotropy. The right Cauchy-Green tensor ***C*** is therefore an appropriate

strain measure:

$$\boldsymbol{C} = \boldsymbol{F}^T \cdot \boldsymbol{F} \tag{6}$$

The fibres behave linearly elastic. The free energy $\boldsymbol{\Psi}$ of the fibres then equals the elastic stored energy [1]:

$$\boldsymbol{\Psi} = \frac{E_f}{8\rho_0 \ell_0^4}(\boldsymbol{C}-\boldsymbol{I}) : \boldsymbol{a}_0\boldsymbol{a}_0\boldsymbol{a}_0\boldsymbol{a}_0 : (\boldsymbol{C}-\boldsymbol{I}) \tag{7}$$

where E_f denotes the fibre stiffness and ρ_0 the stress-free density of the material. The local stress now reads:

$$\boldsymbol{\tau} = \frac{\rho E_f \ell^2}{2\rho_0 \ell_0^6} \boldsymbol{a}_0\boldsymbol{a}_0\boldsymbol{a}_0\boldsymbol{a}_0 : (\boldsymbol{C}-\boldsymbol{I}) \tag{8}$$

and the Cauchy stress:

$$\boldsymbol{\sigma} = \frac{\rho E_f}{2\rho_0 \ell_0^4} \boldsymbol{a}\boldsymbol{a}\boldsymbol{a}_0\boldsymbol{a}_0 : (\boldsymbol{C}-\boldsymbol{I}) \tag{9}$$

This large deformation formulation of the fibre model can be extended to an arbitrary anisotropic elastic model.

$$\boldsymbol{\tau} = \frac{\rho}{2\rho_0}\left(\boldsymbol{G} \cdot {}^4I \cdot \boldsymbol{G}^T\right) : {}^4\boldsymbol{E} : (\boldsymbol{C}-\boldsymbol{I}) \tag{10}$$

with ${}^4\boldsymbol{E}$ is the invariant and constant fourth order material tensor. ${}^4\boldsymbol{I}$ is a fourth order tensor and has the property ${}^4\boldsymbol{I} : \boldsymbol{A}=\boldsymbol{A}$, where $\boldsymbol{A}$ is an arbitrary second order tensor.

2.3 Parallel fraction model

The model consists of several material fractions. Deformation is equal for each fraction and each fraction contributes to the total stress proportional to its volume fraction *v*.

$$\boldsymbol{\sigma} = \sum_i v_i \boldsymbol{\sigma}_i \tag{11}$$

where *i* denotes the fraction number and the sum of the volume fractions equals unity. This allows for implementation of several deformation mechanisms into one model, as shown in ten Thije et al. [4].

2.4 Consistent tangent matrix

The performance of implicit FE simulations depends largely on the consistency of the tangent (stiffness) matrix when using a Newton-Raphson procedure. The iterative process converges very slow or even diverges if not **all** the nonlinearities are taken into account, especially when it concerns highly anisotropic materials.

The time derivative of the weak mechanical equilibrium equation can be derived from the virtual power and reads:

$$\begin{aligned}\int_\Omega \boldsymbol{w}\overleftarrow{\nabla} : \dot{\boldsymbol{\sigma}}\, d\Omega - \int_\Omega \boldsymbol{w}\overleftarrow{\nabla}\cdot\boldsymbol{v}\overleftarrow{\nabla} : \boldsymbol{\sigma}\, d\Omega + \\ \int_\Omega \boldsymbol{w}\overleftarrow{\nabla} : \boldsymbol{\sigma}\, tr(\boldsymbol{D})\, d\Omega = \int_\Gamma \boldsymbol{w}\cdot\dot{\boldsymbol{t}}\, d\Gamma\end{aligned} \tag{12}$$

where $\boldsymbol{w}$ are the element weighting functions, $\boldsymbol{v}$ is the velocity and $\boldsymbol{D}$ is the rate of deformation tensor. Using the constitutive model for the fibres and ignoring the surface traction part this can be rewritten to:

$$\begin{aligned}\int_\Omega \left\{\frac{E_f\rho}{\rho_0\ell_0^4}\left(\tfrac{1}{2}\left(\boldsymbol{w}\overleftarrow{\nabla}+\overrightarrow{\nabla}\boldsymbol{w}\right)\cdot\boldsymbol{a}\boldsymbol{a}\right) : \left(\boldsymbol{a}\boldsymbol{a}\cdot\tfrac{1}{2}\left(\boldsymbol{v}\overleftarrow{\nabla}+\overrightarrow{\nabla}\boldsymbol{v}\right)\right)\right\} d\Omega + \\ \int_\Omega \overrightarrow{\nabla}\boldsymbol{w}\cdot\boldsymbol{v}\overleftarrow{\nabla} : \boldsymbol{\sigma}\, d\Omega = 0\end{aligned} \tag{13}$$

The time derivative when using the generalized anisotropic material model of equation (10) reads:

$$\begin{aligned}\int_\Omega \left\{\frac{\rho}{\rho_0}\tfrac{1}{2}\left(\boldsymbol{w}\overleftarrow{\nabla}+\overrightarrow{\nabla}\boldsymbol{w}\right) : \left(\boldsymbol{F}\cdot{}^4\boldsymbol{I}\cdot\boldsymbol{F}\right) : {}^4\boldsymbol{E} : \left(\boldsymbol{F}^T\cdot{}^4\boldsymbol{I}\cdot\boldsymbol{F}^T\right) : \right. \\ \left. \tfrac{1}{2}\left(\boldsymbol{v}\overleftarrow{\nabla}+\overrightarrow{\nabla}\boldsymbol{v}\right)\right\} d\Omega + \int_\Omega \overrightarrow{\nabla}\boldsymbol{w}\cdot\boldsymbol{v}\overleftarrow{\nabla} : \boldsymbol{\sigma}\, d\Omega = 0\end{aligned} \tag{14}$$

3 APPLICATION: BIAS EXTENSION

The large deformation FE formulation was implemented in Matlab to examine the performance. The bias extension experiment is a suitable test case for the simulation performance. This experiment was extensively described by Potter [5]. Figure 5 shows the undeformed and the deformed shape. The biaxial fabric is gripped on the short edges and pulled apart. The fabric develops three deformation regions: an undeformed region, a central region with pure shear and a region with intermediate shear. The mesh is aligned with the fibre directions to avoid intra ply shear locking. Reduced integration of quadrilaterals or higher order elements appears to be effective as well, but gives rise to hourglass deformation modes. This is in line with the work of Yu et al. [6].

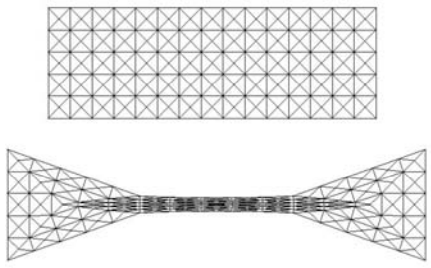

Fig. 5. The undeformed and deformed shape of the bias extension simulation (no displacement scaling).

The deformation shown in figure 5 is applied in only one step, which is a remarkable good performance for an implicit FE code. Figure 6 shows the

convergence behaviour of this simulation.

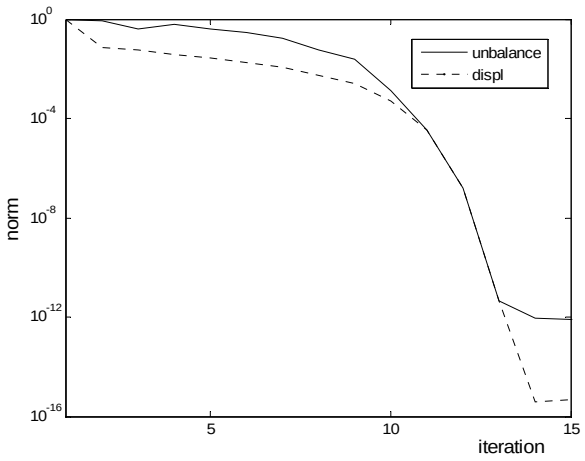

Fig. 6. Convergence plot of the one-step bias extension simulation from figure 5.

The unbalance norm is given by $\|R\text{-}F\|/\|F\|$ and the displacement norm by $\|\Delta u\|/\|u\|$, where R are the reaction forces, F the applied nodal loads, Δu the displacement found during the iteration and u the total displacement. The simulation initially converges slowly, due to strain increments over 100% and fibre rotations up to 45°. After 8 iterations it shows quadratic convergence. All individual steps converge to machine precision within 6 iterations if the simulation is split into more than 3 steps, showing quadratic convergence from the first iteration on.

Another large advantage of the nonlinear Cauchy Green strain definition is the increased robustness of the simulation when using poorly shaped elements. Figure 5 shows elements with angles below 2°, but the simulation can be continued with another step without problems.

3.1 Numerical issues

Figure 6 shows a displacement norm that gets down to machine precision. The unbalance norm remains 10^3 times higher. This is due to the condition of the system. The fibre stiffness is 10^3 times higher than the bulk stiffness, causing unbalances in the same order of magnitude.

Care should be taken when storing the deformation gradient. Large rounding errors can occur if deformations are small. $\boldsymbol{F}$ can be written as $\boldsymbol{I} + \boldsymbol{\delta F}$ and significant digits of $\boldsymbol{\delta F}$ are lost when storing $\boldsymbol{F}$. This causes inaccuracy if the local stress $\boldsymbol{\tau}$ is evaluated (*equation 8*). Subtraction of $\boldsymbol{I}$ then results in inaccurate strains due to the lost significant digits. Storing $\boldsymbol{\delta F}$ instead of $\boldsymbol{F}$ and rewriting the strain definition in terms of $\boldsymbol{\delta F}$ solves this problem and does not lead to large numerical rounding errors if small deformations are applied.

4 CONCLUSIONS

The standard FE codes are not very suitable for large deformation simulations of highly anisotropic materials. It leads to confusing formulations as well. To avoid misalignment of the nodal forces, the material axis of anisotropy should be evaluated on the final geometry. However, this causes the accuracy of the strain prediction to drop significantly.

Instead, the deformation gradient is decomposed into a rotation tensor and a stretch tensor. The rotation reflects the rotation of the axis of anisotropy. This is an advantage when modelling fibre reinforced composites. Stresses are computed using invariant local stress and stiffness tensors. This leads to a simple and straightforward implementation of constitutive laws, which do not have to account for any rotation of the material.

Consistent tangent matrices are given for linearly elastic fibres and for a generalized anisotropic material. Simulations converge quadratically for arbitrary deformation gradients and arbitrary degrees of anisotropy. Simulations are far more robust than the standard implementations. Using the right Cauchy Green strain definition causes badly shaped element to behave much better than when using a linear strain definition.

The scheme is implemented and tested in 2D simulations. The next step is to test the behaviour the new scheme in a full 3D forming simulation.

REFERENCES

1. J.Huétink, *On Anisotropy, Objectivity and Invariancy in finite thermo-mechanical deformations*. Proceedings on the 9th International ESAFORM Conference on Material Forming, 2006.
2. Woong-Ryeol Yu, Philip Harrison and Andrew Long, *Finite element forming simulation for non-crimp fabrics using a non-orthogonal constitutive equation*, Composites Part A: Applied Science and Manufacturing, Volume 36, Issue 8, August 2005, Pages 1079-1093
3. Pu Xue, Xiongqi Peng and Jian Cao, *A non-orthogonal constitutive model for characterizing woven composites*, Composites Part A: Applied Science and Manufacturing, Volume 34, Issue 2, February 2003, Pages 183-193
4. R.H.W. ten Thije, R. Loendersloot and R. Akkerman, Material characterisation for finite element simulation of draping with non-crimp fabrics, *Proceedings on the 6th International ESAFORM Conference on Material Forming*, Nuova Ipsa Editore, Palermo (2003), 859-862.
5. Kevin Potter, *Bias extension measurements on cross-plied unidirectional prepreg*, Composites: Part A 33 (2002), p. 63-73
6. Xiaobo Yu, Bruce Cartwright, Damian McGuckin, Lin Ye and Yiu-Wing Mai, *Intra-ply shear locking in finite element analyses of woven fabric forming processes*, Composites Part A: Applied Science and Manufacturing, In Press.